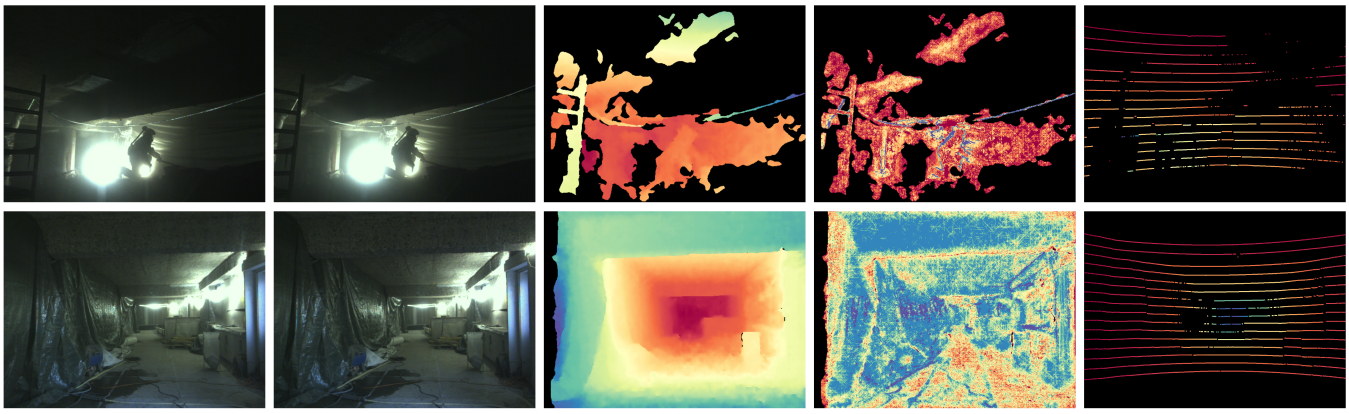
arXiv:2606.23152v1 [cs.RO] 22 Jun 2026

ShotcreteDepth: A Bi-modal Dataset for Robust Robotic Depth Perception in Shotcrete Construction Environments

Jakub Gregorek[1,2*], Lars Arnold Dethlefsen[1,2], Patrick Schmidt[1,2],
Mads Essenbæk[3], Jonas Flink Bentzen[3] and Lazaros Nalpantidis[1,2]



(a) RGB Left (b) RGB Right (c) Disparity (d) Confidence (e) LiDAR

Fig. 1: **Data samples from our *ShotcreteDepth* dataset.** RGB images originate from Roboception rc_visard 160c camera, the disparity and confidence is computed internally by the camera, and point cloud from the Velodyne LiDAR projected to the image plane. Red color denotes the smallest and blue the largest values.

***Abstract*— We introduce *ShotcreteDepth*, a bi-modal dataset from the construction domain that captures both an active shotcreting process and general construction environments. The dataset comprises stereo RGB imagery and LiDAR point clouds acquired under harsh real-world conditions, including high turbidity and poor illumination. Such conditions adversely affect sensor measurements, leading to incomplete and noisy observations that pose significant challenges for perception systems in autonomous applications. Alongside the dataset, we release a lightweight annotation tool designed for time-efficient labeling of LiDAR point clouds. ShotcreteDepth consists of 11,252 temporally synchronized data samples, of which 220 are annotated for evaluation purposes. The dataset supports research in stereo matching, depth completion, and depth estimation under conditions that closely reflect the operational complexities found in industrial settings. Project repository: https://github.com/dtu-pas/shotcrete-depth**

I. Introduction

We are publishing a bi-modal dataset—*ShotcreteDepth*—capturing a shotcreting environment, shown in Fig. 1, aimed at development and evaluation of stereo matching, depth completion and depth estimation methods. Furthermore, we are releasing a light-weight annotation tool for LiDAR point clouds. The application of sprayed concrete, "shotcrete", is a construction method which can be used for reinforcing unstable structures in underground mining or tunnel constructions, building complex geometries or repairing damaged structures. The technology is mechanized to the large extend, yet the shotcrete application is still laborious work performed manually. The motivation to automate this process is rooted in achieving more consistent quality, ensuring compliance with the design requirements, reducing material and water waste by eliminating over-spraying, and limiting exposure of human workers to harmful quick-setting agents [33]. The full automation of the shotcreting process has many aspects [2], [12], [19], [27], [48], [49], [67], [68], one of which is advanced perception for autonomous systems, which are to perform the application of shotcrete. This work is aimed at the depth perception, which is relevant for navigation, mapping, obstacle avoidance, safety, measuring material deposition, compliance and process monitoring. The shotcreting environment, characterized by turbidity, poses a challenge for robotic perception systems. The rebound phenomenon produces significant amount of airborne shotcrete dust concentrating in the enclosed environments. The dust limits the visibility, negatively impacting camera based depth sensing, and causes laser scattering, challenging active depth sensors like LiDARs. Development of reliable perception systems for the construction site domain, even more so for

[1]Technical University of Denmark, Department of Electrical and Photonics Engineering. [2]Pioneer Centre for AI, Copenhagen, Denmark. [3]Christiansen & Essenbæk A/S. *Corresponding author jagre@dtu.dk. This work has been funded and supported by the EU Horizon Europe project "RoBétArmé" under the Grant Agreement 101058731. We express our gratitude to Søren Beyer Nielsen for designing and 3D printing the dust-proof sensor housing.

niche applications like shotcrete, suffer from lack of data. The contributions of this paper are twofold and aiming to narrow this gap:

- We are releasing a shotcreting dataset capturing a niche construction environment with the emphasis on depth perception. We are using this dataset to test various stereo, depth completion, and depth estimation baselines to elucidate its characteristics.
- We are providing a light-weight annotation tool for 3D point clouds allowing users to label unreliable depth measurements.

TABLE I: ***ShotcreteDepth*** **dataset parameters.**

Parameter	Description/Value
Stereo Camera	Roboception rc_visard 160 color
– Field of View	Horizontal: 61°, Vertical: 48°
– Image Resolution	1280×960
– Disparity Resolution	640×480
LiDAR	Velodyne PUCK
– Field of View	Vertical: 30°
– Depth Resolution	1280×960
Total Dataset Size	11252
Annotated Dataset Size	220

II. Related Work

A. Relevant Datasets

Only a few construction-related datasets contain any form of depth data, but they target a variety of tasks: SLAM [55], segmentation [11], [22], [24], [30], place recognition [34], pose estimation [61], 3D reconstruction [22], object detection [11], depth estimation [11]. When it comes to shotcreting or tasks related to the shotcreting process, existing datasets aim at segmentation [50], structural performance [54] and deformations [10]. Similar harsh environmental conditions to a certain extent, including turbidity, haziness, excessive or insufficient illumination can be observed in [1], [6], [13]. To our knowledge, there is no existing dataset capturing the niche shotcreting domain allowing development and evaluation of depth perception methods such as depth estimation, completion and stereo matching.

B. Depth Estimation

Depth estimation is the task of estimating depth based on a provided monocular image. Considering the data scarcity in this niche field, our interest is mainly on the methods that, have been evaluated in the zero-shot context. Ranftl et al. [47] pioneered the zero-shot monocular depth estimation. Many of the recent depth estimation models are based on Vision Transformer (ViT) backbones [7], [37], [45], [46], [57], [58], [65], [66] initialized from DINOv2 [43], and pre-trained ConvNext and ResNet backbones [47], [69]. Others methods take the generative approach [14], [18], [20], [28], [62], [70], [70]. The depth estimation models may predict disparity [20], [47], [65], [66], relative depth estimates [18], [28], [37], [57], [62], [70], metric depth [5], [7], [45], [46], [58], [69], or can be fine-tuned for metric depth [37], [65], [66]. Whereas real-world labeled datasets are usually required to train the depth estimation models [45]–[47], [69], some methods can take advantage of unlabeled data [37], [65], [66] and recently synthetic datasets have also started playing an important role [7], [18], [20], [28], [45], [57], [58], [62], [70].

C. Depth Completion

In the context of this paper we define depth completion to be the task of densifying sparse depth, guided by a monocular image. Zero-shot capable depth completion methods may benefit from the pre-trained priors of the depth estimators [16], [17], [23], [25], [29], [39], [51], [56] or stereo matching architectures [3]. Some of the recent state-of-the-art methods formulate the problem as test-time optimization. Ke et al. [29] applies low-rank adaptation and visual prompt tuning. Prompt tuning was also explored by Jeong et al. [25] and low-rank adaptation by Seo et al. [51]. Diffusion-based methods [16], [23], [56] use the sparse depth to iteratively guide the diffusion process. Faster inference compared to the test-time optimization can be achieved by fine-tuning the diffusion model [17]. In contrast, Bartolomei et al. [3] utilizes virtual pattern projector and re-trains stereo matching network [40] achieving strong zero-shot generalization. Liang et al. [35] proposes a distillation framework leveraging supervision of the strong depth estimators, whereas Lin et al. [39] performs super-resolution targeting noisy low-resolution sensors. Finally, Zuo and Deng [71] proposes an approach based on gated recurrent units iteratively refining depth gradients, depth integration and SPN enhancement. That work was further extended [72] introducing multi-resolution depth integrator and Laplacian loss.

D. Stereo Matching

Stereo matching is the task of finding correspondences between images captured by a stereo camera allowing to estimate depth of the observed scene. While Semi-Global Matching by Hirschmüller [21] became an industrial standard due to its favorable accuracy-efficiency trade-off [42], the deep learning methods have dominated the task. Some of the methods aggregate cost volume [31], [52], [53], [64], which is often memory expensive. Other methods perform recurrent disparity refinement [8], [36], [40], [63], which is less time-efficient. An alternative approach avoiding the construction of a cost-volume is utilizing attention mechanisms establishing correspondences between stereo images [59]. The most recent methods combine the mentioned approaches [4], [26], [60] and simultaneously take advantage of the monocular foundational depth models [43], [66].

III. Dataset

A. Overview

Our dataset captures the environment where the shotcreting is performed, including scenes before, during and after shotcreting, as well as the general construction environment. The dataset is bi-modal, aiming to provide data for development and evaluation of depth perception systems

in conditions with challenging environmental conditions, including high turbidity and far-from-optimal illumination. It contains 11,252 temporally synchronized data samples, of which 220 are annotated for evaluation purposes. Selection of the evaluation set maximizes diversity, skipping similar consecutive frames. An overview of the dataset's parameters are presented in Tab. I.

B. Environment

The construction site at which the dataset was collected exemplifies the type of environment autonomous systems will need to operate in, should this demanding task be automated. The workspace was sealed off from the outside, so illumination was provided exclusively by artificial lighting, and shotcrete particles accumulated rapidly in the air. The construction environments are often confined, as shotcreting is commonly done in tunnels or mines. These factors together create particularly harsh conditions for both human workers and equipment. To protect the sensors from shotcreting particles, they were mounted inside a custom 3D-printed dust-proof sensor housing, shown in Fig. 3.

C. Sensors & Modalities

Our bi-modal dataset was captured using two sensors: Roboception rc_visard 160c stereo camera with 4mm lens and Velodyne PUCK LiDAR. The stereo camera provides RGB images of resolution 1280×960 pixels, disparity and confidence maps of resolution 640×480, which are computed by proprietary implementation of Semi-Global Matching [21] running directly on the Nvidia Tegra K1 embedded in the camera. The Velodyne PUCK LiDAR measures depth up to 100m with typical accuracy up to $\pm 3cm$. The LiDAR has 16 scan lines, vertical field of view of 30°, and operates on 903nm wavelength. The LiDAR was mounted approximately centered above the stereo camera in our dust resistant housing. We have also performed tests with a solid-state LiDAR Neuvition Titan M1 (visible at the bottom of Fig. 3, which did not seem to be well suited for this task. It struggled in the turbid environment to the extent of being unable to return any depth whatsoever. It could be explained by the longer wave-length (1550nm) it operates with or internal processing not being tuned for these conditions.

D. Calibration & Synchronization

The intrinsic camera parameters were estimated using the Roboception's calibration tool which is built in the camera. The extrinsic parameters of the camera and LiDAR were obtained using Matlab's Camera LiDAR and Camera Calibration. The accurate LiDAR time-stamping was ensured by the PPS signal and NMEA messages received from a GPS module. The camera's clock was synchronized using PTP with a system clock of our acquisition computer (also synchronized with GPS time). Our sensor setup acquires the modalities at different frequencies: RGB images at 25Hz, stereo disparity at 3Hz and LiDAR point clouds at 10 Hz. The RGB images and disparity from the stereo camera were matched with the temporally closest point cloud producing only complete sets containing all modalities (cf. Fig. 1).

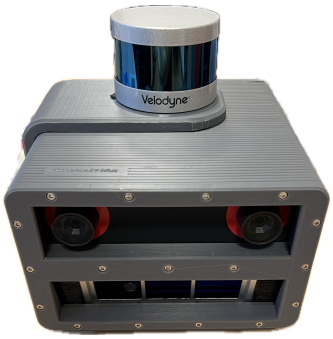


Fig. 3: Our 3D printed dust-proof sensor housing containing the Roboception rc_visard 160 stereo camera and the Velodyne PUCK LiDAR.

E. Influence of Turbidity

Visibility worsens in turbid environments, which typically makes stereo matching more difficult. Nevertheless, LiDAR seems to be affected more severely and the shotcrete particles dispersed in the air seem to degrade the quality of depth measurements in situations with reasonable visibility. The impact on LiDAR is three-fold:

1) *Missing data.* The large amount of shotcrete particles in the air may "blind" the LiDAR either partially or even entirely.
2) *Noisy measurements.* Point clouds become visually more noisy during shotcreting.
3) *Dust clouds.* Shotcrete particles become visible in the LiDAR point clouds, while being mostly translucent for the camera and human eyes.

F. Point Cloud Annotation Tool

We developed an annotation tool, allowing us to manually annotate the dust clouds of shotcrete observed by the LiDAR. The tool allows the user to assign each point in the point cloud a "kept by user" or "removed by user" label. Additionally we define the labels "kept by algorithm" and "removed by algorithm", which are to be used for annotations performed programmatically. The user interface consists of two views (depicted in Fig. 4): the first view displays the LiDAR point cloud in 3D, whereas the second view displays the projection of the point cloud on top of the left RGB picture. The user can switch modes using shortcuts to rotate or annotate the displayed point cloud following the selected operation, keeping or removing the points. Furthermore, the tool allows the user to flag the image for evaluation. We annotated only the point clouds of the dataset samples that are to be used for evaluation. The remaining point clouds are provided without annotations.

G. Removing Occlusions

Utilizing multiple sensors to capture the same scene inevitably leads to occlusions [9]. To filter out occluded LiDAR points we follow [3]. That method uses a sliding window, that moves on top of the depth points projected to the image plane. Points at a larger distance than the nearest

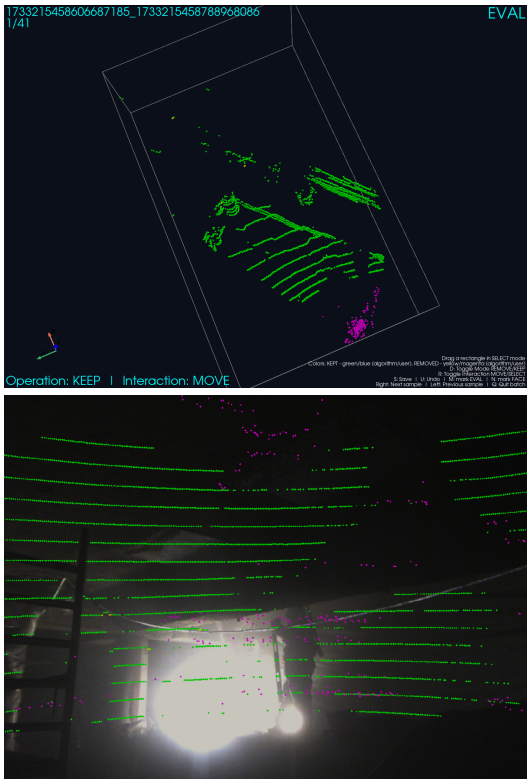


Fig. 4: **The Annotation Tool** we are releasing with the dataset. Upper image: 3D view of the LiDAR point cloud. Lower image: point cloud overlaid on top of the left camera image. The green points are "kept" while the purple color denotes the dust cloud which is to be excluded from evaluation data.

point contained in the sliding window by a given threshold are removed. Considering the lower amount of LiDAR scan lines compared to [15], we enlarge the sliding window to 10×50 pixels and set the distance threshold to 0.5m. The points marked for removal by the user are ignored in the process because removal of valid points projected in the proximity of the dust clouds is not desired. The points to be removed by the filtering method are marked as "removed by algorithm" in the provided annotations.

IV. Experiments

We used the *ShotcreteDepth* dataset ourselves to test various stereo, depth completion, and depth estimation baselines. The goal of these experiments was to elucidate the characteristics of the dataset.

A. Experimental Setup

For all evaluated methods, inference was performed at a resolution of 640×480 pixels. The predictions were then upscaled and metrics computed at the original resolution of 1280×960. The annotated and filtered LiDAR point clouds serve as the ground-truth for model evaluation. The depth completion models were provided 500 uniformly sampled depth points C originating from stereo matching. The same depth points were also used to align scale a and shift b of the affine-invariant predictions D of the depth estimation models. The alignment was performed by minimizing the least square error:

$$(a, b) = \arg\min_{a,b} \sum_{i \in \Omega} (a\, D_i + b - C_i)^2 \tag{1}$$

The evaluation of stereo matching models requires ground-truth depth to be converted to disparity. Furthermore, disparity originating from the stereo matching needs to be converted to depth for sampling the sparse depth maps for the depth completion methods. This can be achieved by the formula:

$$depth = \frac{baseline \times focal\ length}{disparity} \tag{2}$$

where the baseline is given by the stereo setup and focal length is determined in the camera calibration process.

B. Metrics

Following the standard practices, for depth estimation models we report absolute relative error REL $= \frac{1}{N}\sum_i |\frac{\mathbf{d}_i - \mathbf{g}_i}{\mathbf{g}_i}|$ and δ_1 percentage of points i where $\max\left(\frac{\mathbf{d}_i}{\mathbf{g}_i}, \frac{\mathbf{g}_i}{\mathbf{d}_i}\right) < 1.25$. N denotes count of pixels in an image, $\mathbf{d}_i$ are prediction pixels and $\mathbf{g}_i$ are ground-truth pixels. For depth completion models we report root mean squared error RMSE $= \sqrt{\frac{1}{N}\sum_i |\mathbf{d}_i - \mathbf{g}_i|^2}$ and mean absolute error MAE $= \frac{1}{N}\sum_i |\mathbf{d}_i - \mathbf{g}_i|$. The values of both, RMSE and MAE, are always provided in meters. RMSE and MAE metrics in do not fully capture the model's ability to produce good quality estimates, especially when the ground-truth is sparse. Thus, we also assess boundary accuracy following [32], [44] and report Pseudo Depth Boundary Error (PDBE) accuracy $\mathcal{E}^{\text{acc}}_{\text{PDBE}}$ and completeness $\mathcal{E}^{\text{comp}}_{\text{PDBE}}$. We extract the ground-truth edges for PDBE metrics from stereo matching. For stereo matching methods we report end-point error EPE $= \frac{1}{N}\sum_i |\mathbf{d}_i - \mathbf{g}_i|$ expressed in pixels. The formulaic definition of EPE matches MAE with the exception that the prediction and ground-truth are in disparity space. Additionally, D1 is percentage of elements with error greater than 3 pixels and greater than 5% of the ground-truth disparity. For all evaluated methods we provide runtime in seconds. Timing was performed on Nvidia GeForce 4090. Model sizes are in millions of parameters.

C. Models

For FoundationStereo [60] we evaluated the ViT-Large checkpoint "23-51-11". For StereoAnywhere [4] we utilized the checkpoint pretrained on SceneFlow [41]. For RAFT-Stereo [40] we downloaded the Middlebury checkpoint recommended for in-the-wild images. For Marigold-SSD [17] we use the model trained on density range $[0.16\%, 5\%]$. Marigold-DC [56] utilizes the Marigold [28] v1.0 checkpoint. For VPP4DC [3] we used the model trained from scratch on SceneFlow [41]. For Depth Anything v3 [37], we evaluated GIANT-1.1 checkpoint. Marigold-E2E [14] weights were downloaded from HuggingFace. For MoGe-2 [58] we used ViT-Large checkpoint. The depth image

settings of the rc_visard camera were set to defaults, with the exception of "Quality" being set to "Full" and enabled "Double-Shot" and "Static".

D. Stereo Matching

The quantitative results evaluating the selected stereo matching methods are presented in Tab. II. In Fig. 5 we compare the methods qualitatively. While stereo matching based on Semi-global Matching [21] is optimized enough to run on embedded hardware, it often produces incomplete depth maps. The more computationally heavy-weight neural networks are more robust in the challenging environmental conditions captured in our dataset. We can observe, that the methods based on neural networks can deal with occlusions and provide more visually distinct edges on the object boundaries, even in extremely dark (cf. Fig. 5-left) or overexposed (cf. Fig. 5-middle) parts of images.

E. Depth Completion

The results for depth completion are presented in Tab. III. The depth methods were used to complete depth maps sampled from stereo matching. The Stereo Anywhere method was selected as the source of depth, because it achieves the lowest EPE and D1, which are the common metrics for evaluation of the matching algorithms. 500 depth points were sampled uniformly. Stereo Anywhere was also used as the source of ground-truth edges for PDBE metrics, because it produces visually cleanest output (see Fig. 5). The qualitative results including visualization of the sampled sparse depth are presented in Fig. 6.

F. Depth Estimation

We evaluated three depth estimation models; the results are summarized in Tab. IV. The sparse depth maps sampled for the depth completion methods in the previous subsection were used to align shift and scale of the affine invariant estimates of Depth Anything v3 [38] and Marigold-E2E [14]. Since MoGe-2 [58] predicts metric depth we evaluated it with and without shift and scale adjustment. The qualitative results are presented in Fig. 7.

TABLE II: **Evaluation of stereo matching methods**: three neural-network based approaches (RAFT - RAFT-Stereo [40], FS - FoundationStereo [60], SA - Stereo Anywhere [4]) and the proprietary SGM [21] implementation running on the Roboception rc_visard 160 camera. Timing was performed on Nvidia GeForce 4090, while runtime of the camera's stereo matching given by the FPS of the camera.

Metrics	Methods			
	RAFT	FS	SA	rc_visard
EPE↓	2.449	2.439	2.328	2.276
D1↓	0.130	0.129	0.103	0.106
MAE↓	0.337	0.327	0.311	1.467
RMSE↓	0.729	0.741	0.795	2.207
Coverage	100%	100%	100%	61%
Parameters	11 M	375 M	347 M	-
Runtime	0.141	0.156	0.307	0.333

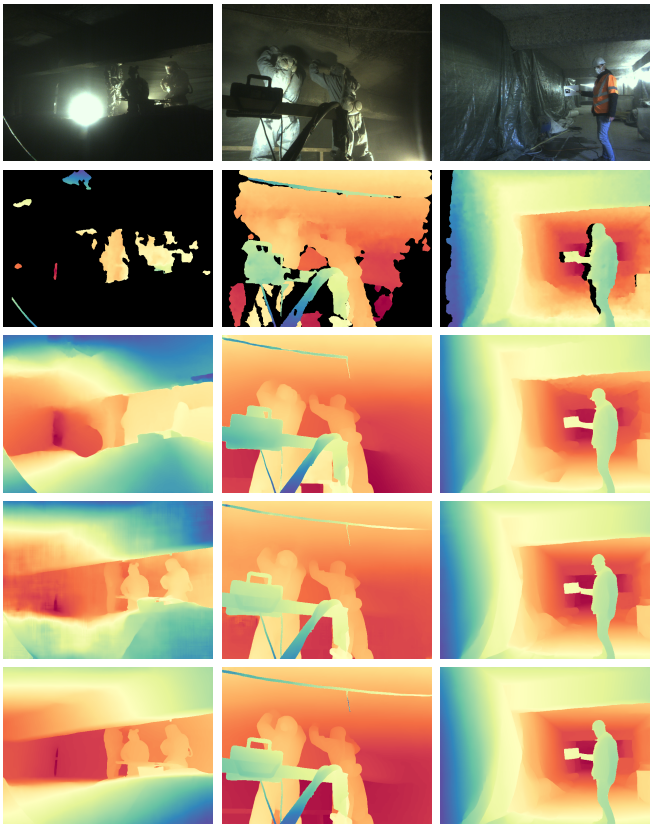


Fig. 5: **Comparing stereo matching methods**. From top to bottom: left RGB image, disparity maps computed by rc_visard stereo matching, RAFT-Stereo [40], Foundation-Stereo [60] and Stereo Anywhere [4].

TABLE III: **Evaluation of three depth completion methods**: Marigold-DC [56] for a single run (1st value) and ensemble of 10 runs (2nd value), Marigold-SSD [17] and VPP4DC [3].

Metrics	Methods		
	Marigold-DC	Marigold-SSD	VPP4DC
MAE↓	0.364 / 0.325	0.422	0.360
RMSE↓	0.893 / 0.793	0.868	0.790
$\mathcal{E}^{\text{acc}}_{\text{PDBE}}$ ↓	1.636 / 1.189	1.576	2.076
$\mathcal{E}^{\text{comp}}_{\text{PDBE}}$ ↓	4.687 / 5.780	21.107	10.783
Parameters	950 M	989 M	11 M
Runtime	24.479 / 254.284	0.382	0.116

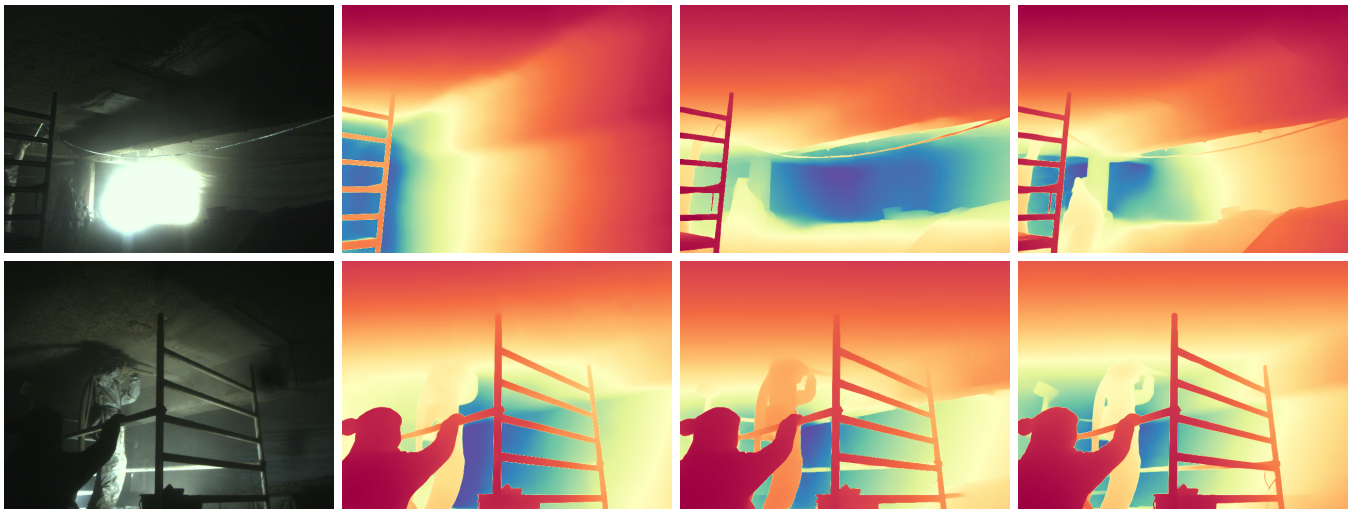
TABLE IV: **Evaluation of depth estimation methods**: DepthAnything v3 [37], Marigold-E2E [14], MoGe-2 [58] with scale and shift alignment (1st value) and without (2nd value).

Metrics	Methods		
	DepthAnything v3	Marigold-E2E	MoGe-2
REL↓	0.133	0.174	0.142 / 0.210
δ_1 ↑	0.834	0.727	0.816 / 0.594
MAE↓	0.554	0.715	0.576 / 0.832
RMSE↓	0.852	1.016	0.879 / 1.134
Parameters	1356 M	950 M	326 M
Runtime	0.095	0.175	0.057



(a) RGB (b) Sparse Depth (c) Marigold-SSD (d) Marigold-DC (e) VPP4DC

Fig. 6: **Qualitative results for depth completion methods.**



(a) RGB (b) Marigold-E2E (c) Depth Anything v3 (d) MoGe-2

Fig. 7: **Qualitative results for depth estimation methods.**

V. Discussion and Conclusion

Our experiments in Sec. IV, have shown that depth perception is indeed possible in the challenging conditions of shotcreting environments. Each one of the tested approaches—3 stereo matching approaches, 3 depth completion methods and 3 depth estimation methods—has exhibited merits in the corresponding task. While computational efficiency and near-real-time operation is feasible, this comes at the expense of output accuracy. Contrary, large deep learning-based models are characterized by inferior runtimes (even when executed on dedicated GPU-enabled workstations), but their accuracy is typically growing with their size for all 3 considered tasks.

In this work, we have introduced *ShotcreteDepth*, a bimodal dataset for evaluation and development of depth perception methods and used it to test 9 state-of-the-art deep learning methods. Our dataset captures the niche shotcreting environment; an environment characterized by high turbidity. Additionally, we developed a lightweight annotation tool for 3D point clouds, which used to remove the dust clouds observed by LiDAR from the evaluation. Stereo cameras and LiDARs are fundamentally distinct and better suited for different scenarios. We see a potential to achieve the best depth perception by their fusion, which would require an additional source of depth for evaluation.

References

[1] Codruta O. Ancuti, Cosmin Ancuti, Mateu Sbert, and Radu Timofte. Dense-Haze: A Benchmark for Image Dehazing with Dense-Haze and Haze-Free Images. In *2019 IEEE International Conference on Image Processing (ICIP)*, pages 1014–1018, 2019.

[2] Sotirios Barlakas, Dimitrios Alexiou, Kosmas Tsiakas, Dimitrios Katsatos, Ioannis Kostavelis, Dimitrios Giakoumis, Antonios Gasteratos, and Dimitrios Tzovaras. Robot active vision-based path planning for localization improvement in indoor environments. In *2024 IEEE/RSJ International Conference on Intelligent Robots and Systems (IROS)*, pages 10686–10693. IEEE, 2024.

[3] Luca Bartolomei, Matteo Poggi, Andrea Conti, Fabio Tosi, and Stefano Mattoccia. Revisiting Depth Completion from a Stereo Matching Perspective for Cross-domain Generalization . In *2024 International Conference on 3D Vision (3DV)*, pages 1360–1370, Los Alamitos, CA, USA, Mar. 2024. IEEE Computer Society.

[4] Luca Bartolomei, Fabio Tosi, Matteo Poggi, and Stefano Mattoccia. Stereo Anywhere: Robust Zero-Shot Deep Stereo Matching Even Where Either Stereo or Mono Fail. pages 1013–1027, 2025.

[5] Shariq Farooq Bhat, Reiner Birkl, Diana Wofk, Peter Wonka, and Matthias Müller. ZoeDepth: Zero-shot Transfer by Combining Relative and Metric Depth, 2023.

[6] Mario Bijelic, Tobias Gruber, Fahim Mannan, Florian Kraus, Werner Ritter, Klaus Dietmayer, and Felix Heide. Seeing Through Fog Without Seeing Fog: Deep Multimodal Sensor Fusion in Unseen Adverse Weather. In *The IEEE Conference on Computer Vision and Pattern Recognition (CVPR)*, June 2020.

[7] Aleksei Bochkovskii, Amaël Delaunoy, Hugo Germain, Marcel Santos, Yichao Zhou, Stephan R Richter, and Vladlen Koltun. Depth Pro: Sharp Monocular Metric Depth in Less Than a Second. *arXiv preprint arXiv:2410.02073*, 2024.

[8] Ziyang Chen, Wei Long, He Yao, Yongjun Zhang, Bingshu Wang, Yongbin Qin, and Jia Wu. MoCha-Stereo: Motif Channel Attention Network for Stereo Matching. In *Proceedings of the IEEE/CVF Conference on Computer Vision and Pattern Recognition (CVPR)*, pages 27768–27777, June 2024.

[9] Andrea Conti, Matteo Poggi, Filippo Aleotti, and Stefano Mattoccia. Unsupervised confidence for LiDAR depth maps and applications. In *2022 IEEE/RSJ International Conference on Intelligent Robots and Systems (IROS)*, pages 8352–8359, 2022.

[10] Li-Zhuang Cui, Jian Liu, Hongzheng Luo, Jianhong Wang, Xiao Zhang, Gaohang Lv, and Quanyi Xie. Deformation measurement of tunnel shotcrete liner using the multiepoch LiDAR point clouds. *Journal of Construction Engineering and Management*, 150(6):04024049, 2024.

[11] Yuexiong Ding and Xiaowei Luo. A virtual construction vehicles and workers dataset with three-dimensional annotations. *Engineering Applications of Artificial Intelligence*, 133:107964, 2024.

[12] Yurui Du, Louis Hanut, Herman Bruyninckx, and Renaud Detry. AREPO: Uncertainty-Aware Robot Ensemble Learning Under Extreme Partial Observability. *IEEE Robotics and Automation Letters*, 10(6):5737–5744, 2025.

[13] Kangkang Duan, Zehao Zhu, and Zhengbo Zou. Indoor FireRescue Radar: 4D Indoor Millimeter Wave Dataset and Analysis for Hazardous Environment Perception. In *2025 IEEE/RSJ International Conference on Intelligent Robots and Systems (IROS)*, pages 18620–18627, 2025.

[14] Gonzalo Martin Garcia, Karim Abou Zeid, Christian Schmidt, Daan de Geus, Alexander Hermans, and Bastian Leibe. Fine-Tuning Image-Conditional Diffusion Models is Easier than You Think. In *Proceedings of the Winter Conference on Applications of Computer Vision (WACV)*, pages 753–762, February 2025.

[15] Andreas Geiger, Philip Lenz, Christoph Stiller, and Raquel Urtasun. Vision meets Robotics: The KITTI Dataset. *International Journal of Robotics Research (IJRR)*, 2013.

[16] Jakub Gregorek and Lazaros Nalpantidis. SteeredMarigold: Steering Diffusion Towards Depth Completion of Largely Incomplete Depth Maps. In *2025 IEEE International Conference on Robotics and Automation (ICRA)*, pages 13304–13311, 2025.

[17] Jakub Gregorek, Paraskevas Pegios, Nando Metzger, Konrad Schindler, Theodora Kontogianni, and Lazaros Nalpantidis. Need for Speed: Zero-Shot Depth Completion with Single-Step Diffusion, 2026.

[18] Ming Gui, Johannes Schusterbauer, Ulrich Prestel, Pingchuan Ma, Dmytro Kotovenko, Olga Grebenkova, Stefan Andreas Baumann, Vincent Tao Hu, and Björn Ommer. DepthFM: Fast Generative Monocular Depth Estimation with Flow Matching. In *Proceedings of the AAAI Conference on Artificial Intelligence*, volume 39, pages 3203–3211, 2025.

[19] Louis Hanut, Yurui Du, Andrew Vande Moere, Renaud Detry, and Herman Bruyninckx. Robotic Framework for Iterative and Adaptive Profile Grading of Sand. In *2025 IEEE International Conference on Robotics and Automation (ICRA)*, pages 10387–10393, 2025.

[20] Jing He, Haodong Li, Wei Yin, Yixun Liang, Leheng Li, Kaiqiang Zhou, Hongbo Zhang, Bingbing Liu, and Ying-Cong Chen. Lotus: Diffusion-based Visual Foundation Model for High-quality Dense Prediction. In *The Thirteenth International Conference on Learning Representations*, 2025.

[21] H. Hirschmuller. Accurate and efficient stereo processing by semi-global matching and mutual information. In *2005 IEEE Computer Society Conference on Computer Vision and Pattern Recognition (CVPR'05)*, volume 2, pages 807–814 vol. 2, 2005.

[22] Shangfeng Huang, Ruisheng Wang, and Xin Wang. BuildingWorld: A Structured 3D Building Dataset for Urban Foundation Models. *Proceedings of the AAAI Conference on Artificial Intelligence*, 40(7):5085–5094, Mar. 2026.

[23] Lee Hyoseok, Kyeong Seon Kim, Kwon Byung-Ki, and Tae-Hyun Oh. Zero-shot Depth Completion via Test-time Alignment with Affine-invariant Depth Prior. *Proceedings of the AAAI Conference on Artificial Intelligence*, 39(4):3877–3885, Apr. 2025.

[24] Muhammad Ibrahim, Naveed Akhtar, Michael Wise, and Ajmal Mian. Annotation Tool and Urban Dataset for 3D Point Cloud Semantic Segmentation. *IEEE Access*, 9:35984–35996, 2021.

[25] Chanhwi Jeong, Inhwan Bae, Jin-Hwi Park, and Hae-Gon Jeon. Test-Time Prompt Tuning for Zero-Shot Depth Completion. In *Proceedings of the IEEE/CVF International Conference on Computer Vision (ICCV)*, pages 9443–9454, October 2025.

[26] Hualie Jiang, Zhiqiang Lou, Laiyan Ding, Rui Xu, Minglang Tan, Wenjie Jiang, and Rui Huang. DEFOM-Stereo: Depth Foundation Model Based Stereo Matching. In *IEEE International Conference on Computer Vision and Pattern Recognition (CVPR)*, 2025.

[27] Dimitrios Katsatos, Paschalis Charalampous, Patrick Schmidt, Ioannis Kostavelis, Dimitrios Giakoumis, Lazaros Nalpantidis, and Dimitrios Tzovaras. Semantic 3D Reconstruction for Volumetric Modeling of Defects in Construction Sites. *Robotics*, 13(7), 2024.

[28] Bingxin Ke, Anton Obukhov, Shengyu Huang, Nando Metzger, Rodrigo Caye Daudt, and Konrad Schindler. Repurposing Diffusion-Based Image Generators for Monocular Depth Estimation. In *Proceedings of the IEEE/CVF Conference on Computer Vision and Pattern Recognition (CVPR)*, 2024.

[29] Bingxin Ke, Qunjie Zhou, Jiahui Huang, Xuanchi Ren, Tianchang Shen, Konrad Schindler, Laura Leal-Taixé, and Shengyu Huang. Depth Completion as Parameter-Efficient Test-Time Adaptation, 2026.

[30] Maximilian Kellner, Mariana Ferrandon Cervantes, Yuandong Pan, Ruodan Lu, Ioannis Brilakis, and Alexander Reiterer. SemanticBridge—A dataset for 3D semantic segmentation of bridges and domain gap analysis. *Developments in the Built Environment*, 26:100912, 2026.

[31] Alex Kendall, Hayk Martirosyan, Saumitro Dasgupta, Peter Henry, Ryan Kennedy, Abraham Bachrach, and Adam Bry. End-To-End Learning of Geometry and Context for Deep Stereo Regression. In *Proceedings of the IEEE International Conference on Computer Vision (ICCV)*, Oct 2017.

[32] Tobias Koch, Lukas Liebel, Friedrich Fraundorfer, and Marco Korner. Evaluation of CNN-based Single-Image Depth Estimation Methods. In *Proceedings of the European Conference on Computer Vision (ECCV) Workshops*, pages 0–0, 2018.

[33] I Kostavelis, L Nalpantidis, R Detry, H Bruyninckx, A Billard, S Christian, M Bosch, K Andronikidis, H Lund-Nielsen, P Yosefipor, U Wajid, R Tomar, FL Martínez, F Fugaroli, D Papargyriou, N Mehandjiev, G Bhullar, E Gonçalves, J Bentzen, M Essenbæk, C Cremona, M Wong, M Sanchez, D Giakoumis, and D Tzovaras. RoBétArmé Project: Human-robot collaborative construction system for shotcrete digitization and automation through advanced perception, cognition, mobility and additive manufacturing skills [version 1; peer review: 1 approved, 2 approved with reservations]. *Open Research Europe*, 4(4), 2024.

[34] Dongjae Lee, Minwoo Jung, and Ayoung Kim. ConPR: Ongoing Construction Site Dataset for Place Recognition, 2024.

[35] Yingping Liang, Yutao Hu, Wenqi Shao, and Ying Fu. Distilling Monocular Foundation Model for Fine-grained Depth Completion. In *Proceedings of the IEEE/CVF Conference on Computer Vision and Pattern Recognition (CVPR)*, pages 22254–22265, June 2025.

[36] Zhaohuai Liang and Changhe Li. Any-stereo: Arbitrary scale disparity estimation for iterative stereo matching. In *Proceedings of the AAAI Conference on Artificial Intelligence*, volume 38, pages 3333–3341, 2024.

[37] Haotong Lin, Sili Chen, Junhao Liew, Donny Y. Chen, Zhenyu Li, Guang Shi, Jiashi Feng, and Bingyi Kang. Depth Anything 3: Recovering the Visual Space from Any Views, 2025.

[38] Haotong Lin, Sili Chen, Jun Hao Liew, Donny Y. Chen, Zhenyu Li, Guang Shi, Jiashi Feng, and Bingyi Kang. Depth Anything 3: Recovering the visual space from any views. *arXiv preprint arXiv:2511.10647*, 2025.

[39] Haotong Lin, Sida Peng, Jingxiao Chen, Songyou Peng, Jiaming Sun, Minghuan Liu, Hujun Bao, Jiashi Feng, Xiaowei Zhou, and Bingyi Kang. Prompting Depth Anything for 4K Resolution Accurate Metric Depth Estimation. In *Proceedings of the IEEE/CVF Conference on Computer Vision and Pattern Recognition (CVPR)*, pages 17070–17080, June 2025.

[40] Lahav Lipson, Zachary Teed, and Jia Deng. RAFT-Stereo: Multilevel Recurrent Field Transforms for Stereo Matching. In *2021 International conference on 3D vision (3DV)*, pages 218–227. IEEE, 2021.

[41] Nikolaus Mayer, Eddy Ilg, Philip Hausser, Philipp Fischer, Daniel

Cremers, Alexey Dosovitskiy, and Thomas Brox. A Large Dataset to Train Convolutional Networks for Disparity, Optical Flow, and Scene Flow Estimation. In *Proceedings of the IEEE Conference on Computer Vision and Pattern Recognition (CVPR)*, June 2016.

[42] Lazaros Nalpantidis, Georgios Ch. Sirakoulis, and Antonios Gasteratos. Review of stereo vision algorithms: from software to hardware. *International Journal of Optomechatronics*, 2(4):435–462, 2008.

[43] Maxime Oquab, Timothée Darcet, Théo Moutakanni, Huy Vo, Marc Szafraniec, Vasil Khalidov, Pierre Fernandez, Daniel Haziza, Francisco Massa, Alaaeldin El-Nouby, Mahmoud Assran, Nicolas Ballas, Wojciech Galuba, Russell Howes, Po-Yao Huang, Shang-Wen Li, Ishan Misra, Michael Rabbat, Vasu Sharma, Gabriel Synnaeve, Hu Xu, Hervé Jegou, Julien Mairal, Patrick Labatut, Armand Joulin, and Piotr Bojanowski. DINOv2: Learning Robust Visual Features without Supervision, 2024.

[44] Duc-Hai Pham, Tung Do, Phong Nguyen, Binh-Son Hua, Khoi Nguyen, and Rang Nguyen. SharpDepth: Sharpening Metric Depth Predictions Using Diffusion Distillation. In *Proceedings of the Computer Vision and Pattern Recognition Conference*, pages 17060–17069, 2025.

[45] Luigi Piccinelli, Christos Sakaridis, Yung-Hsu Yang, Mattia Segu, Siyuan Li, Wim Abbeloos, and Luc Van Gool. UniDepthV2: Universal Monocular Metric Depth Estimation Made Simpler. *IEEE Transactions on Pattern Analysis and Machine Intelligence*, 48(3):2354–2367, 2026.

[46] Luigi Piccinelli, Yung-Hsu Yang, Christos Sakaridis, Mattia Segu, Siyuan Li, Luc Van Gool, and Fisher Yu. UniDepth: Universal Monocular Metric Depth Estimation. In *Proceedings of the IEEE/CVF Conference on Computer Vision and Pattern Recognition (CVPR)*, pages 10106–10116, June 2024.

[47] René Ranftl, Katrin Lasinger, David Hafner, Konrad Schindler, and Vladlen Koltun. Towards Robust Monocular Depth Estimation: Mixing Datasets for Zero-Shot Cross-Dataset Transfer. *IEEE Transactions on Pattern Analysis and Machine Intelligence*, 44(3):1623–1637, 2022.

[48] Khadija Sabiri, Luís Afonso, Caio Camargo, Estefânia Gonçalves, and Rui Fernandes. A Virtual Reality-Based Learning Environment for Human—Robot Collaboration Training in Construction 4.0. In *2025 International Conference on Robotic Computing and Communication (RoboticCC)*, pages 54–61, 2025.

[49] Patrick Schmidt, Dimitrios Katsatos, Dimitrios Alexiou, Ioannis Kostavelis, Dimitrios Giakoumis, Dimitrios Tzovaras, and Lazaros Nalpantidis. Towards autonomous shotcrete construction: semantic 3D reconstruction for concrete deposition using stereo vision and deep learning. In *Proceedings of the 41st International Symposium on Automation and Robotics in Construction*, pages 896–903, Lille, France, June 2024. International Association for Automation and Robotics in Construction (IAARC).

[50] Patrick Schmidt and Lazaros Nalpantidis. Segmentation dataset for reinforced concrete construction. *Automation in Construction*, 171:105990, 2025.

[51] Minseok Seo, Wonjun Lee, Jaehyuk Jang, and Changick Kim. Efficient Test-Time Optimization for Depth Completion via Low-Rank Decoder Adaptation, 2026.

[52] Zhelun Shen, Yuchao Dai, and Zhibo Rao. CFNet: Cascade and Fused Cost Volume for Robust Stereo Matching. In *Proceedings of the IEEE/CVF Conference on Computer Vision and Pattern Recognition (CVPR)*, pages 13906–13915, June 2021.

[53] Zhelun Shen, Yuchao Dai, Xibin Song, Zhibo Rao, Dingfu Zhou, and Liangjun Zhang. PCW-Net: Pyramid Combination and Warping Cost Volume for Stereo Matching. In Shai Avidan, Gabriel Brostow, Moustapha Cissé, Giovanni Maria Farinella, and Tal Hassner, editors, *Computer Vision – ECCV 2022*, pages 280–297, Cham, 2022. Springer Nature Switzerland.

[54] Andreas Sjölander, Erik Nordström, and Anders Ansell. Dataset for evaluation and numerical modelling of structural performance of fibre-reinforced shotcrete with fibres of steel, synthetic and basalt. *Data in Brief*, 61:111684, 2025.

[55] Maciej Trzeciak, Kacper Pluta, Yasmin Fathy, Lucio Alcalde, Stanley Chee, Antony Bromley, Ioannis Brilakis, and Pierre Alliez. ConSLAM: Periodically Collected Real-World Construction Dataset for SLAM and Progress Monitoring. In Leonid Karlinsky, Tomer Michaeli, and Ko Nishino, editors, *Computer Vision – ECCV 2022 Workshops*, pages 317–331, Cham, 2023. Springer Nature Switzerland.

[56] Massimiliano Viola, Kevin Qu, Nando Metzger, Bingxin Ke, Alexander Becker, Konrad Schindler, and Anton Obukhov. Marigold-DC: Zero-Shot Monocular Depth Completion with Guided Diffusion. In *Proceedings of the IEEE/CVF International Conference on Computer Vision (ICCV)*, pages 5359–5370, October 2025.

[57] Ruicheng Wang, Sicheng Xu, Cassie Dai, Jianfeng Xiang, Yu Deng, Xin Tong, and Jiaolong Yang. MoGe: Unlocking Accurate Monocular Geometry Estimation for Open-Domain Images with Optimal Training Supervision. In *Proceedings of the IEEE/CVF Conference on Computer Vision and Pattern Recognition (CVPR)*, pages 5261–5271, June 2025.

[58] Ruicheng Wang, Sicheng Xu, Yue Dong, Yu Deng, Jianfeng Xiang, Zelong Lv, Guangzhong Sun, Xin Tong, and Jiaolong Yang. MoGe-2: Accurate Monocular Geometry with Metric Scale and Sharp Details. In *The Thirty-ninth Annual Conference on Neural Information Processing Systems*, 2025.

[59] Philippe Weinzaepfel, Thomas Lucas, Vincent Leroy, Yohann Cabon, Vaibhav Arora, Romain Brégier, Gabriela Csurka, Leonid Antsfeld, Boris Chidlovskii, and Jérôme Revaud. Croco v2: Improved cross-view completion pre-training for stereo matching and optical flow. In *Proceedings of the IEEE/CVF International Conference on Computer Vision*, pages 17969–17980, 2023.

[60] Bowen Wen, Matthew Trepte, Joseph Aribido, Jan Kautz, Orazio Gallo, and Stan Birchfield. FoundationStereo: Zero-Shot Stereo Matching. In *Proceedings of the IEEE/CVF Conference on Computer Vision and Pattern Recognition (CVPR)*, pages 5249–5260, June 2025.

[61] Chao Xie and Aladdin Alwisy. Advancing robotic automation in wood-framed construction using vision-driven adaptive control. *Automation in Construction*, 185:106858, 2026.

[62] Gangwei Xu, Haotong Lin, Hongcheng Luo, Xianqi Wang, Jingfeng Yao, Lianghui Zhu, Yuechuan Pu, Cheng Chi, Haiyang Sun, Bing Wang, Guang Chen, Hangjun Ye, Sida Peng, and Xin Yang. Pixel-Perfect Depth with Semantics-Prompted Diffusion Transformers, 2025.

[63] Gangwei Xu, Xianqi Wang, Xiaohuan Ding, and Xin Yang. Iterative geometry encoding volume for stereo matching. In *Proceedings of the IEEE/CVF conference on computer vision and pattern recognition*, pages 21919–21928, 2023.

[64] Haofei Xu and Juyong Zhang. AANet: Adaptive Aggregation Network for Efficient Stereo Matching. In *Proceedings of the IEEE/CVF Conference on Computer Vision and Pattern Recognition (CVPR)*, June 2020.

[65] Lihe Yang, Bingyi Kang, Zilong Huang, Xiaogang Xu, Jiashi Feng, and Hengshuang Zhao. Depth Anything: Unleashing the Power of Large-Scale Unlabeled Data. In *Proceedings of the IEEE/CVF Conference on Computer Vision and Pattern Recognition (CVPR)*, pages 10371–10381, June 2024.

[66] Lihe Yang, Bingyi Kang, Zilong Huang, Zhen Zhao, Xiaogang Xu, Jiashi Feng, and Hengshuang Zhao. Depth Anything V2. In A. Globerson, L. Mackey, D. Belgrave, A. Fan, U. Paquet, J. Tomczak, and C. Zhang, editors, *Advances in Neural Information Processing Systems*, volume 37, pages 21875–21911. Curran Associates, Inc., 2024.

[67] Mohammad Reza Yazdi Samadi, Ralf Waspe, and Christian Schlette. Physics-based particle system modeling of shotcrete process for robotic placement. *Construction Robotics*, 9(2):30, 2025.

[68] Mohammad Reza Yazdi Samadi, Rui Wu, Soheil Gholami, Ralf Waspe, Ali Muhammad, Aude Billard, and Christian Schlette. From Human to Height-Field: Predictive Shotcrete Simulation with a Physics-Informed Particle System. In *2025 IEEE International Conference on Advanced Robotics (ICAR)*, pages 826–832, 2025.

[69] Wei Yin, Chi Zhang, Hao Chen, Zhipeng Cai, Gang Yu, Kaixuan Wang, Xiaozhi Chen, and Chunhua Shen. Metric3D: Towards Zero-shot Metric 3D Prediction from A Single Image. In *Proceedings of the IEEE/CVF International Conference on Computer Vision (ICCV)*, pages 9043–9053, October 2023.

[70] Xiang Zhang, Bingxin Ke, Hayko Riemenschneider, Nando Metzger, Anton Obukhov, Markus Gross, Konrad Schindler, and Christopher Schroers. BetterDepth: Plug-and-Play Diffusion Refiner for Zero-Shot Monocular Depth Estimation. In A. Globerson, L. Mackey, D. Belgrave, A. Fan, U. Paquet, J. Tomczak, and C. Zhang, editors, *Advances in Neural Information Processing Systems*, volume 37, pages 108674–108709. Curran Associates, Inc., 2024.

[71] Yiming Zuo and Jia Deng. OGNI-DC: Robust Depth Completion with Optimization-Guided Neural Iterations. In *Computer Vision – ECCV 2024*, pages 78–95, Cham, 2025. Springer Nature Switzerland.

[72] Yiming Zuo, Willow Yang, Zeyu Ma, and Jia Deng. OMNI-DC: Highly Robust Depth Completion with Multiresolution Depth Integration. In *Proceedings of the IEEE/CVF International Conference on Computer Vision (ICCV)*, pages 9287–9297, October 2025.